AMERICAN SOCIETY FOR MICROBIOLOGY | Journal of Virology

A Novel Open and Infectious Form of Echovirus 1

Mira Myllynen, Artur Kazmertsuk, Varpu Marjomäki

Department of Biological and Environmental Science, Nanoscience Center, University of Jyväskylä, Jyväskylä, Finland

ABSTRACT

One of the hallmarks of enterovirus genome delivery is the formation of an uncoating intermediate particle. Based on previous studies of mostly heated picornavirus particles, intermediate particles were shown to have externalized the innermost capsid protein (VP4) and exposed the N terminus of VP1 and to have reduced infectivity. Here, in addition to the native and intact particle type, we have identified another type of infectious echovirus 1 (E1) particle population during infection. Our results show that E1 is slightly altered during entry, which leads to the broadening of the major virion peak in the sucrose gradient. In contrast, CsCl gradient separation revealed that in addition to the light intact and empty particles, a dense particle peak appeared during infection in cells. When the broad peak from the sucrose gradient was subjected to a CsCl gradient, it revealed light and dense particles, further suggesting that the shoulder represents the dense particle. The dense particle was permeable to SYBR green II, it still contained most of its VP4, and it was able to bind to its receptor $\alpha_2\beta_1$ integrin and showed high infectivity. A thermal assay further showed that the $\alpha_2\beta_1$ integrin binding domain (I-domain) stabilized the virus particle. Finally, heating E1 particles to superphysiological temperatures produced more fragile particles with aberrant ultrastructural appearances, suggesting that they are distinct from the dense E1 particles. These results describe a more open and highly infectious E1 particle that is naturally produced during infection and may represent a novel form of an uncoating intermediate.

IMPORTANCE

In this paper, we have characterized a possible uncoating intermediate particle of E1 that is produced in cells during infection. Before releasing their genome into the host cytosol, enteroviruses go through structural changes in their capsid, forming an uncoating intermediate particle. It was shown previously that structural changes can be induced by receptor interactions and, in addition, by heating the native virion to superphysiological temperatures. Here, we demonstrate that an altered, still infectious E1 particle is found during infection. This particle has a more open structure, and it cannot be formed by heating. It still contains the VP4 protein and is able to bind to its receptor and cause infection. Moreover, we show that in contrast to some other enteroviruses, the receptor-virion interaction has a stabilizing effect on E1. This paper highlights the differences between enterovirus species and further increases our understanding of various uncoating forms of enteroviruses.

Picornaviruses are a large family of pathogens infecting humans and animals across the globe. The vast disease range caused by these viruses spans from simple rashes to paralysis and meningitis. It has been estimated that approximately half of the seasonal common-cold cases reported are caused by rhinoviruses, members of the family subgroup *Enterovirus* (1). Increased emphasis on enterovirus research is caused by the evidence associating type I diabetes, asthma, and myocarditis with members of the enterovirus genus (2–4).

Echovirus 1 (E1), a member of the enterovirus B group, shares the structural characteristics of all picornaviruses: a positive-sense single-stranded RNA genome of ~7,500 nucleotides with a nonenveloped capsid of roughly 30 nm in size that is comprised of four noncovalently interacting viral proteins (VP1, VP2, VP3, and VP4). During the course of picornavirus entry and uncoating, a common sequence of events has been suggested based on poliovirus and rhinovirus studies: the initial receptor-virion interaction on the cell surface begins the conversion of the native virion to an A-particle (altered particle; also termed a 135S particle due to its sediment coefficient in sucrose) (5, 6). Compared to the native virion, the 135S particle has its VP1 N-terminal segment externalized and has lost its inner capsid protein VP4. Both of these changes are thought to be linked with the membrane-virion interaction and possible pore formation by myristylated VP4 (7–9). The altered particles still hold the genome inside the capsid shell, but recent evidence regarding rhinovirus and coxsackievirus B3 (CVB3) indicates that the RNA-capsid interaction is altered (10, 11). Additionally, an opening forms at the 2-fold axis of the 135S particle, which facilitates the genome's egress from the capsid (12–17). The generation of genome-free, empty (80S) particles occurs only after internalization to an endosome compartment, where the final step(s) of picornavirus uncoating is supposed to take place.

In addition to the native (160S), altered (135S), and empty (80S) particle types described above, poliovirus, coxsackievirus B5, swine vesicular disease virus, and bovine enterovirus were shown to band as two separate particle populations in CsCl. In general, the reported buoyant density profiles vary between 1.34 and 1.47 g cm^{-3}, where the major, intact component is usually found to be less dense than the minor component (18, 19, 20). The reported properties of the dense particles, with respect to the native 160S virion, indicate a similar RNA-to-protein ratio but in-

Received 23 February 2016 **Accepted** 26 April 2016

Accepted manuscript posted online 18 May 2016

Citation Myllynen M, Kazmertsuk A, Marjomäki V. 2016. A novel open and infectious form of echovirus 1. J Virol 90:6759–6770. doi:10.1128/JVI.00342-16.

Editor: S. López, Instituto de Biotecnologia/UNAM

Address correspondence to Varpu Marjomäki, varpu.s.marjomaki@jyu.fi.

creased permeability, often reduced infectivity, and increased RNase and protease sensitivity (19, 21, 22). The origin of dense picornavirus particles has been attributed to increased RNA-cesium interactions due to increased permeability to Cs^+ ions (19). While there are clear structural differences between the native particles and A-particles, the relationship between dense particles and A-particles is rarely discussed.

We have shown that E1 induces a macropinocytic entry pathway that has no connections to the conventional acidic clathrin pathway (23–26). E1 accumulates, together with its receptor $\alpha_2\beta_1$ integrin, in nonacidic multivesicular structures that do not label for endosomal proteins found in classical endosomes (25, 27). Interestingly, members of the same enterovirus group B viruses, such as coxsackievirus A9 (CVA9) (28, 29), CVB3, and coxsackievirus B1 (M. Martikainen, A. S. Khojine, H. Hyöty, and V. Marjomäki, unpublished data), show remarkably similar entry characteristics (30). The present data concerning E1 and CVA9 suggest that, in contrast to poliovirus and rhinovirus, binding to their cell surface receptors, $\alpha_2\beta_1$ and $\alpha_v\beta_3$ integrins, respectively, stabilizes the viruses and that uncoating starts only later, gradually after 30 min postinfection (p.i.) in endosomes (15, 23, 28, 31, 32). It therefore seems that the enterovirus group B viruses have similarities in terms of uncoating and genome release from the endosomes and that these aspects may differ from those of poliovirus and rhinovirus.

In this study, we show that E1 does not show a typical transition into a 135S particle during infection but instead goes through smaller structural alterations that cause only small changes in the sedimentation profile in the sucrose gradient. Additionally, we report the densities of E1 particles in the CsCl gradient and identify a previously undescribed dense E1 particle. This dense particle is formed during infection, and it corresponds to the appearance of a shoulder next to intact E1 particles in the sucrose gradient and thus may represent an uncoating intermediate. The dense particle is highly infectious, permeable to small molecules like SYBR green II (SGII), VP4 positive, and capable of receptor interaction. Finally, we show that heating E1 to superphysiological temperatures causes the formation of more fragile, structurally aberrant particles that are distinct from the naturally formed dense particles that are produced in cells during infection.

MATERIALS AND METHODS

Cells, antibodies, and reagents. Cell experiments were carried out with green monkey kidney (GMK) cells, which were obtained from the American Type Culture Collection (ATCC). The following antibodies were used in the experiments: rabbit polyclonal antibody against E1 (23) and secondary goat anti-rabbit antibody conjugated with Alexa Fluor 555 (Molecular Probes, Invitrogen USA).

The glutathione *S*-transferase (GST)–I-domain fusion was a kind gift from Jyrki Heino (University of Turku). Polyethylene glycol 6000, sodium deoxycholate, and a Nonidet P-40 substitute were obtained from Sigma-Aldrich. Eagle's minimum essential medium (MEM), fetal bovine serum (FBS), GlutaMAX, and penicillin-streptomycin antibiotics were obtained from Gibco, Life Technologies.

Virus preparations. Monolayers of GMK cells were infected with E1 (Farouk strain; ATCC) (multiplicity of infection [MOI] of 0.1) for 24 h in 5-layer bottles, after which the cells were collected and lysed via three freeze-thaw cycles. Cell debris was pelleted by centrifugation with a JA-10 rotor (6,080 rpm for 30 min), after which the protein obtained from the supernatant was precipitated by adding polyethylene glycol 6000 (final concentration, 8% [wt/vol]) and NaCl (2.2% [wt/vol]). After overnight precipitation at +4°C, the precipitated material was centrifuged with a JA-10 rotor (8,000 rpm for 45 min), and the pellet was dissolved into R buffer (10 mM Tris-HCl [pH 7.5], 200 mM NaCl, 50 mM $MgCl_2$, 10% [wt/vol] glycerol). To disrupt membranous structures, 0.3% (wt/vol) sodium deoxycholate and 0.6% (vol/vol) Nonidet P-40 substitute were added to the suspension, and the mixture was incubated for 30 min on ice. Membrane debris was pelleted via centrifugation with a TX-200 rotor (4,000 × *g* for 15 min), and the supernatant was divided on top of two 10-ml linear 10 to 40% (wt/vol) sucrose gradients made in R buffer. The gradients were ultracentrifuged with an SW-41 rotor (30,000 rpm for 3 h) and fractioned into 500-μl aliquots from the top. The optical density at 260 nm was measured with a NanoDrop 1000 spectrophotometer (Thermo Scientific) to identify virus-containing fractions, and subsequently, three fractions from each gradient were collected for isopycnic centrifugation in 24% CsCl gradients (10 ml) made in TNE buffer (50 mM Tris [pH 7.5], 100 mM NaCl, 1 mM EDTA). The gradients were ultracentrifuged with an SW-41 rotor (30,000 rpm for 24 h) and fractioned into 500-μl aliquots from the top, and the optical density at 260 nm was measured with a NanoDrop 1000 spectrophotometer (Thermo Scientific) to identify virus-containing fractions.

Before further studies, the virus-containing light and dense fractions were dialyzed separately with a Spectra/Por Micro Float-A-Lyzer instrument with Biotech cellulose ester membranes (Spectrum Laboratories Inc., USA). A dialysis column with a 300-kDa-molecular-mass cutoff was prepared according to the instructions provided by the manufacturer, after which the viruses were dialyzed against 2 mM $MgCl_2$–phosphate-buffered saline (PBS). The buffer was changed after 2 and 4 h, after which the sample was dialyzed overnight. Viruses were concentrated via ultracentrifugation with a 70Ti rotor (35,000 rpm for 2 h), and the pellets were dissolved into 2 mM $MgCl_2$–PBS.

In the case of double-CsCl-gradient purification (Fig. 1Aii), the first purification steps were carried out as described above, and the first round of CsCl purification was carried out after pelleting the membranous debris. Before the second CsCl gradient centrifugation, the collected virus fractions were dialyzed with a Spectra/Por Micro Float-A-Lyzer with Biotech cellulose ester membranes (Spectrum Laboratories Inc., USA). The protein content was estimated from the optical density at 260 nm, as described above.

The radioactive virus was produced in monolayers of GMK cells, which were washed with PBS for 15 min at +37°C and infected with E1 (Farouk strain; ATCC) diluted in low-methionine-cysteine medium supplemented with 1% FBS. After 3 h of infection, 50 μCi ml^{-1} of [^{35}S]methionine-cysteine diluted in low-methionine-cysteine medium supplemented with 1% FBS was added. Infection was allowed to proceed for 24 h at +37°C, after which the cells were collected and lysed via freeze-thaw cycles. The cell debris was pelleted via centrifugation with a TX-200 rotor (3,000 × *g* for 15 min), and the supernatant was collected and incubated with 0.3% (wt/vol) sodium deoxycholate and 0.6% (vol/vol) Nonidet P-40 substitute for 30 min on ice. The membrane structures were pelleted via centrifugation with a TX-200 rotor (4,000 × *g* for 15 min), after which the supernatant was added on top of 40% sucrose cushions (2 ml). The cushions were ultracentrifuged with an SW-41 rotor at 30,000 rpm for 2.5 h, after which the liquid above the cushion and one 500-μl fraction were discarded, while the next three 500-μl fractions were collected. The virus-containing fractions were then ultracentrifuged with an SW-41 rotor (30,000 rpm for 24 h) in 24% CsCl gradients (10 ml) made in TNE buffer. The gradients were fractioned into 500-μl aliquots from the top, and the virus-containing fractions were identified via liquid scintillation counting (PerkinElmer).

Light radioactive E1 was added to cells and bound on ice for 1 h. Infection was allowed to proceed at +37°C for the indicated amount of time (0, 30, 120, or 180 min). The cells were lysed by adding 100 mM octyl-β-D-glucopyranoside (Amresco) on ice, and after 30 min of incubation, the virus-containing cell lysate was collected, added either on top of a 10-ml linear 5 to 20% sucrose gradient in R buffer (35,000 rpm for 2 h) or in a 10-ml gradient of 24% CsCl in TNE buffer (30,000 rpm for 24 h),

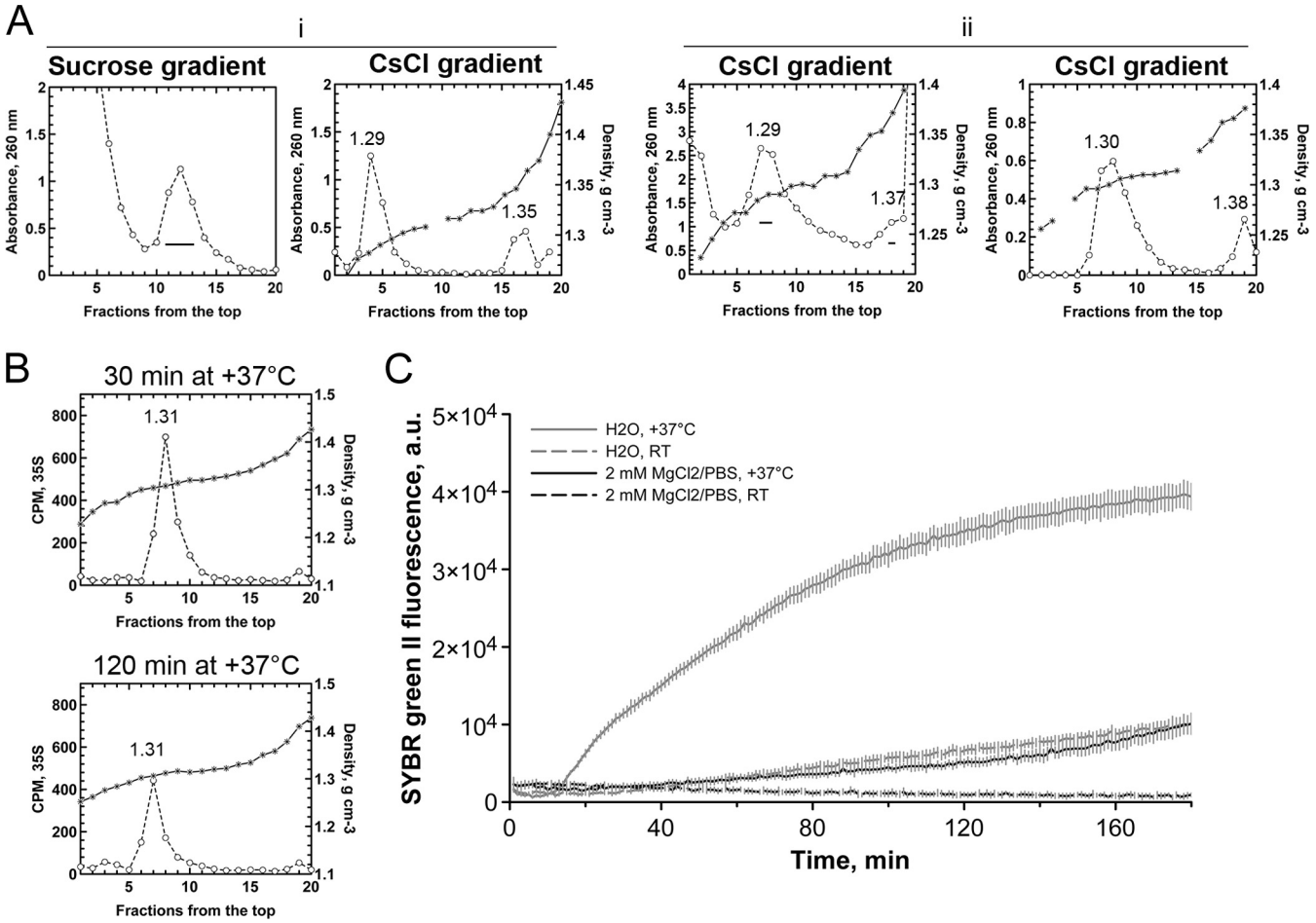

FIG 1 Detection of dense particles in CsCl gradients. (A) Gradient profiles of E1 purified with either a 10 to 40% sucrose-to-CsCl or CsCl-to-CsCl combination. (i) Fractions 11, 12, and 13 (indicated by a line) were collected from the sucrose gradient, mixed, and subjected to the CsCl gradient. (ii) Fractions 7, 8, and 18 (indicated by lines) were collected from the CsCl gradient, mixed, and subjected to a second CsCl gradient. (B) CsCl gradient profile of the *in vitro* conversion of native, light E1 into dense particles after 30 min or 120 min of incubation at +37°C. (C) Real-time measurement of SYBR green II fluorescence at +37°C or RT over 180 min in the presence of light E1 in water or storage buffer (2 mM $MgCl_2$–PBS). The fluorescence of the dye is enhanced when bound to RNA, which enables the determination of virus stability upon heating. The results are averages from three replicates (± standard errors of the means). a.u., arbitrary units.

and ultracentrifuged with an SW-41 rotor. The gradients were fractioned into 500-μl aliquots from the top, and the virus-containing fractions were identified via liquid scintillation counting (PerkinElmer).

For heat treatment of the radioactive virus at +50°C, radioactively labeled E1 was produced as described above and purified via a 40% sucrose cushion, followed by concentration with a 70Ti rotor, as described above. E1 was heated at +50°C for 0 min or 5 min and ultracentrifuged with an SW-41 rotor in either a 10-ml linear 5 to 20% sucrose gradient (35,000 rpm for 2 h) or a 24% CsCl gradient (30,000 rpm for 24 h). The gradients were fractioned into 500 aliquots from the top, and the counts per minute of each fraction were measured via liquid scintillation counting (PerkinElmer).

Cytopathic effect assay. The cytopathic effect (CPE) assay was carried out as previously described (33). The CPE assay was carried out in confluent monolayers of GMK cells. Cells were cultivated in MEM supplemented with 10% FBS, 1% GlutaMAX, and 1% penicillin-streptomycin antibiotics on a 96-well microtiter plate for 1 day, after which the cells were infected with light or dense viruses, which were diluted into MEM supplemented with 1% FBS and 1% GlutaMAX. Three protein amounts were used to infect the cells, 10 ng, 1 ng, and 0.1 ng, and additionally, a control cell, without virus, was included. Each sample included four replicates. After 24 h of infection at +37°C, the infected cells were washed extensively with PBS, and the noninfected cell monolayers were stained with a solution containing crystal violet. Excess stain was washed extensively with sterile water, after which the cell monolayers were treated with 100 μl of lysis buffer to elute the crystal violet. Finally, the absorbance of the crystal violet stain was measured at 570 nm with a Victor X4 2030 multilabel reader (PerkinElmer).

In the I-domain inhibition experiment, 10 ng of virus (light or dense) was incubated with different amounts of I-domain (10 ng, 100 ng, 500 ng, or 1,000 ng) for 1 h at +37°C. Confluent monolayers of the GMK cells were infected with a virus–I-domain mix by binding the virus on ice first for 1 h. The excess virus was washed extensively with PBS containing 0.5% bovine serum albumin, after which infection was allowed to proceed in 1% MEM for 24 h at +37°C. Crystal violet staining and absorbance measurements were carried out as described above.

Endpoint dilution assay. The endpoint dilution assay was carried out in monolayers of GMK cells cultured in 96-well microtiter plates for 1 day in MEM supplemented with 10% FBS, 1% GlutaMAX, and 1% penicillin-streptomycin antibiotics. Infection was carried out in cell monolayers with 30% confluence. Cell monolayers were infected with light or dense virus by preparing a dilution series in MEM supplemented with 1% FBS and 1% GlutaMAX, and infection was monitored daily. After 3 days of infection at +37°C, the medium was removed, and the cell monolayers

were stained with 50 μl of crystal violet stain (8.3 mM crystal violet, 45 mM $CaCl_2$, 10% ethanol, 18.5% formalin, and 35 mM Tris base) for 10 min. The excess crystal violet stain was washed extensively with water, after which the infectivity was determined by calculating the number of dyed (noninfected) and nondyed (infected) wells. The 50% tissue culture infective dose ($TCID_{50}$) was calculated by comparing the numbers of infected and uninfected wells for eight replicates of the same virus concentration. The concentration at which half of the wells would be infected was extrapolated ($TCID_{50}$). Finally, the $TCID_{50}$ values of the light and dense viruses were normalized to the respective protein amounts, as determined by measurement of the A_{260}.

Immunolabeling and microscopy. An immunolabeling experiment was carried out in subconfluent monolayers of GMK cells, which were plated onto coverslips 1 day previously. Monolayers of cells were infected with light or dense virus, and a negative control, without any virus, was also included to remove the antibody-induced background signal during imaging.

Cells were infected with three protein amounts, 250 ng, 75 ng, and 23 ng, by diluting the viruses into MEM supplemented with 1% FBS and 1% GlutaMAX. The viruses were bound on cells for 1 h on ice, after which the excess virus was washed extensively with PBS containing 0.5% bovine serum albumin. The cells were incubated in MEM supplemented with 10% FBS, 1% GlutaMAX, and 1% penicillin-streptomycin antibiotics at +37°C for 6 h, after which the cells were fixed with 4% paraformaldehyde for 30 min at room temperature (RT). Before labeling, the cells were permeabilized with 0.2% Triton X-100 for 5 min. Primary rabbit antibody against E1 was added to cells, and the mixture was incubated at RT for 45 min, after which the cells were washed extensively with PBS. Secondary goat anti-rabbit antibody conjugated with Alexa Fluor 555 (Molecular Probes, Invitrogen USA) was added to cells at RT and incubated for 30 min. Finally, the cells were extensively washed with PBS and mounted with Prolong gold antifade reagent supplemented with 4′,6-diamidino-2-phenylindole (DAPI) (Molecular Probes, Life Technologies).

Immunolabeled samples were imaged with an Olympus IX81 microscope with a FluoView-1000 confocal setup. In total, ~300 cells per sample were checked for infection. The nuclei were counted with a segmentation tool embedded in Bioimage XD software, after which infected cells were counted by hand. The number of infected cells was then compared to the total number of cells to obtain the infection percentage.

Electron microscopy. Butwar-coated copper grids were made hydrophilic via glow discharging with an EMS/SC7620 Mini sputter coater according to the instructions provided by the manufacturer. The virus sample was added to the grid and incubated for 15 s, after which the excess virus was blotted with Whatman 3-mm paper. The viruses were negatively stained by adding 1% phosphotungstic acid (in water) (pH 7.4) to the grid for 1 min, after which the excess stain was blotted with Whatman 3-mm paper. Heat-treated E1 was incubated at 50°C for 5 min before it was added to the grid.

For the I-domain experiment, 1 μg of light or dense virus was incubated with or without 1 μg of I-domain at 37°C for 1 h before it was added to the grid. The samples were dried overnight and imaged with a JEM-1400 (JEOL) transmission electron microscope.

Gel electrophoresis. The protein compositions of the ^{35}S-labeled light and dense viruses were analyzed by using a 4 to 12% NuPAGE Bis-Tris gel (Novex, Life Technologies). The proteins were denatured with the gel sample buffer provided by the manufacturer (NuPAGE; Life Technologies) at 100°C before they were loaded onto the gel. The gel was fixed with 40% methanol and 10% acetic acid for 15 min. The fixative was washed with water, after which the gel was treated with an autoradiography enhancer (Enlightning; PerkinElmer) for 15 min. Excess enhancer was washed with water, and the gel was dried at +70°C for 2 h (Gel dryer 583; Bio-Rad), after which the gel was subjected to autoradiography. The quantification of the band intensities was performed with the Image J gel analysis tool.

Thermal stability assays. The thermal stabilities of the light and dense viruses were assayed by using methods described previously by Walter et al. (34). The fluorescence signal was recorded by using a Bio-Rad C1000 thermal cycler, and the final sample mixture contained 1 μg of light or dense E1 and a 10× concentration of SYBR green II (Invitrogen). All samples were equilibrated at 20°C for 10 min before the thermal stability measurements were begun. For the full temperature range scan, the fluorescence signal was recorded at 10-s intervals and 0.5°C increments. Finally, the sample was cooled back to 20°C, at which point the fluorescence reading was recorded again.

In the I-domain assay, the sample mixture contained 100, 500, or 1,000 ng of I-domain; 1 μg of light E1; and a 10× concentration of SYBR green II (Invitrogen). The measurement was carried out as described above.

The real-time measurement of E1 stability at +37°C was carried out by using a Victor X4 2030 multilabel reader (PerkinElmer) with 485-nm and 535-nm excitation and emission filters, respectively. The sample mixture contained a 10× concentration of SYBR green II (Invitrogen) and 1 μg of light E1 in either deionized water or 2 mM $MgCl_2$–PBS. The fluorescence signal was recorded at 1-min intervals, for 180 min in total.

RNase protection assay. Light or dense E1 was incubated with RNase A (final concentration, 25 μg ml^{-1}) for 30 min at RT before the addition of the virus to cells. Infectivity was determined with an endpoint dilution assay, and the $TCID_{50}$ per milliliter was calculated based on eight replicates, as described above. Finally, the $TCID_{50}$ per milliliter was normalized to the A_{260} values of the viruses.

RESULTS

Detection of a dense particle in a CsCl gradient. In order to produce highly purified echovirus 1 for detailed spectroscopic and biochemical studies, we set out to use a combination approach, using both sucrose and CsCl gradients (Fig. 1A). A 10 to 40% sucrose gradient produced a concentrated sample of E1, which was then subjected to a CsCl gradient (Fig. 1Ai). To our surprise, the CsCl gradient repeatedly showed two bands, a light-density fraction on the top part of the gradient and a well-separated dense fraction in the bottom of the gradient. In CsCl, the light E1 population had an apparent buoyant density of 1.29 g cm^{-3}, while the dense particle banded at 1.35 to 1.38 g cm^{-3} (Fig. 1Ai and ii). The purification of the virus in the CsCl gradient, without the previous sucrose gradient step, also produced the same light and dense fractions (Fig. 1Aii). If the light and dense fractions were collected from the gradient, mixed again, and subjected to a second CsCl gradient separation, this reproduced the same separation of the light and dense fractions (now without very light impurities). These results thus suggest that these two density fractions are found in the CsCl gradient independent of whether the first separation was performed on a sucrose or CsCl gradient. It also further showed that CsCl separation does not progressively produce more of the dense fraction during separation, because the two consecutive gradients produced roughly similar ratios of light and dense fractions. In order to rule out the possibility of a contaminating picornavirus in our stock, we also performed similar CsCl banding experiments using the infectious cDNA clone of E1 and observed that both the top and the bottom components were similar to our stock virus (data not shown).

To rule out the effect of temperature on dense-particle formation, the light fraction was incubated at +37°C for 30 min or 120 min before CsCl gradient fractionation (Fig. 1B). The results showed a remarkable stability of the light particles and clearly showed that the physiological temperature did not alone induce dense-particle formation. In addition, a real-time measurement of

particle opening at +37°C based on the fluorescence of RNA binding SYBR green II dye showed that the virus capsid was stable at +37°C in storage buffer (2 mM $MgCl_2$–PBS), in contrast to the virus incubated in water, which showed opening of the virus for SYBR green II binding already after 15 min at +37°C (Fig. 1C). The virus incubated for 180 min at +37°C in buffer was also shown to be infectious (data not shown).

Formation of the E1 dense particle during infection. In order to understand when the dense E1 particle appears during virus infection in cells, a radioactive virus was produced, and cell homogenates were fractioned by CsCl ultracentrifugation at various time points postinfection (Fig. 2A). First, the light top fractions were collected from the CsCl gradient in order to use only the intact form of the virus as an input for the cell experiments. This light fraction was added to cells, and the distribution of the virus was monitored after fractionation (Fig. 2D). CsCl gradient separation showed that the dense particle had already appeared at 30 min p.i., and the population was apparent at later time points as well (Fig. 2A). After 180 min, the proportional amount of the dense fraction had already decreased, probably due to some particle disruption already at this time point. In order to compare more quantitatively the virus particles found inside and outside cells, quantification of the different particles (empty, light, and dense) in a CsCl gradient was performed for the virus gained after incubating the light fraction on cells for 2 h or adding the light fraction straight into the gradient (Fig. 2B). This measurement showed that inside the cells, more than half of the virus particles were of the dense form, while outside cells, over 80% of the virus particles stayed intact. Even if some dense particles may develop spontaneously, these result support the idea that dense-particle formation is not an artifact caused by centrifugation but, instead, is induced in cells.

Since different forms of enteroviruses are often separated by using a sucrose gradient, we also carried out the same infection time series using a 5 to 20% sucrose gradient for separation (Fig. 2C). The light input fraction from the CsCl purification showed a typical peak in fractions 14 to 17 from the top of the sucrose gradient. At 30 min p.i., the peak generated a shoulder or a widened peak, which still became more evident after 120 and 180 min (Fig. 2C). Thus, in the case of E1, a typical transition of the native peak (160S) to the 135S position was not detected in the sucrose gradient over time, but instead, the native peak became broader, as was observed in our previous studies (23). The time course generation of the denser particle in CsCl correlated with the broadening of the native peak in the sucrose gradient, suggesting that the dense virion was inside this broad peak (Fig. 2A and C). When the broad peak (fractions 12 to 16) was collected from the sucrose gradient and subjected to a CsCl gradient (Fig. 2E), both intact (light) particles and dense particles were detected, further confirming that the shoulder in the sucrose gradient corresponded to the dense particle in the CsCl gradient. In repetitions of this approach, the amount of the left-hand shoulder in the sucrose gradient was positively correlated with the amount of the dense peak of the CsCl gradient produced in relation to the light peak. Based on all these data, E1 is marginally altered from the intact virion upon entry, which can be observed by the appearance of a shoulder in the 5 to 20% sucrose gradient and a distinct high-density particle in the CsCl gradient. This may represent the formation of an E1 uncoating intermediate, which is different from many other enteroviruses.

The dense particle is porous and still contains VP4. To further investigate the structural properties of the dense E1 particle, we performed a thermal stability assay using SYBR green II (SGII) as a reporter (34). The sensitivity of SGII for detecting RNA can be attributed to several factors, including superior fluorescence quantum yield, binding affinity, and fluorescence enhancement when bound to RNA. In a thermal assay, SGII is typically added to the virus sample at room temperature. By increasing the temperature by 0.5°C at 10-s intervals, this assay produces a curve from which the melting temperature (T_m) can be deduced (34). The native light virion showed a T_m of 53°C, while the dense particle was already permeable to SGII at room temperature, leading to high starting values. Thus, measurements of the melting temperature of the dense E1 particle were impossible to perform due to the apparent initial permeability of the capsid to SGII (Fig. 3A). The initial versus final fluorescence measurements (Fig. 3A) confirmed that the genomic material was already fully accessible to SGII in the case of the dense E1 particle, while the native virion denied SGII entry initially. This also explained the density of the dense virion and confirmed previous suggestions regarding the formation of dense particles (19): if the dense particle penetrates SGII, it is permeable to Cs ions as well, leading to the density increase seen in the CsCl gradient.

Because the dense particle of E1 was observed to be porous and previous studies suggested that the dense particles were sensitive to RNase A, we also carried out an assay to evaluate the sensitivity of dense and light particles to RNase A (Fig. 3B). The particles were incubated with the enzyme for 30 min at RT before the addition of the virus to the cells. Infectivities were determined with an endpoint dilution assay, which showed that neither the light nor the dense particles were prone to RNase A-mediated digestions. The RNase A-treated fractions were as infectious as the untreated fractions (Fig. 3B).

We next performed an SDS-PAGE analysis on the protein compositions of both the native and the dense E1 particles in order to determine whether VP4 was present in the virus capsids. Radioactive labeling (^{35}S) indeed showed a significant VP4 signal for the dense E1 particle (Fig. 3C). The amount of VP4 was also quantified by measuring the intensities of the bands via Image J. Quantification revealed that the shares of VP4, based on the intensities of all the capsid proteins VP1 to VP4, were 4.5% and 4.3% for the light and dense virions, respectively. The results corresponded well to the theoretical values calculated based on the sequence of E1. Theoretically, the share of methionines and cysteines in VP4 was 4.3% of the total amount of methionines and cysteines in the sequences of the capsid proteins.

Heat-treated virus particles are distinct from the dense particles detected in cells. The uncoating intermediates of picornaviruses for structural studies are commonly produced by heating the native virion at elevated temperatures for several minutes (12, 13, 16, 35, 36). In the case of poliovirus, the cell-derived uncoating intermediates and heat-converted uncoating intermediates were suggested to be indistinguishable from one another (37). E1 virions heated to 50°C for 5 min (in PBS supplemented with 2 mM $MgCl_2$) produced a wide peak in the sucrose gradient compared to the nonheated virions (Fig. 4Ai). However, the shift in the heated virions was different from what was observed when the native virion was incubated on cells (Fig. 2C and E). In addition, when the heat-treated virions were separated by using CsCl, the native virion band at 1.31 g cm^{-3} almost totally disappeared (Fig. 4Aii),

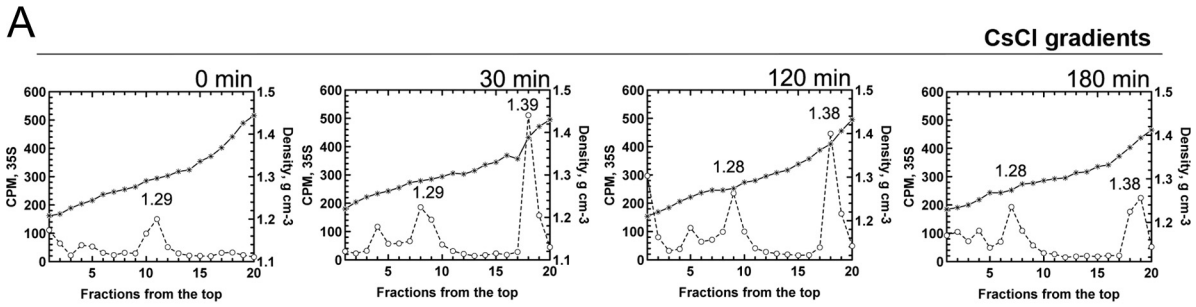

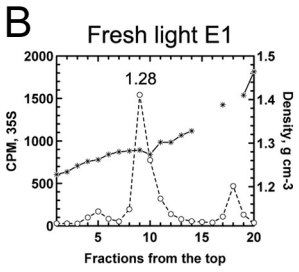

Distribution of particles in CsCl gradient

	Empty E1 (%)	Light E1 (%)	Dense E1 (%)
Light E1 on cells for 2 h	19.7 ± 3.6	24.3 ± 4.9	56.0 ± 2.3
Fresh light E1	5.9 ± 2.8	82.6 ± 4.5	11.6 ± 3.2

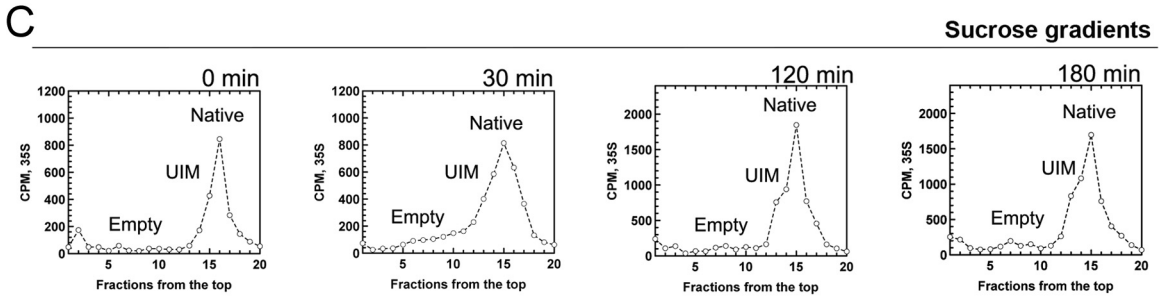

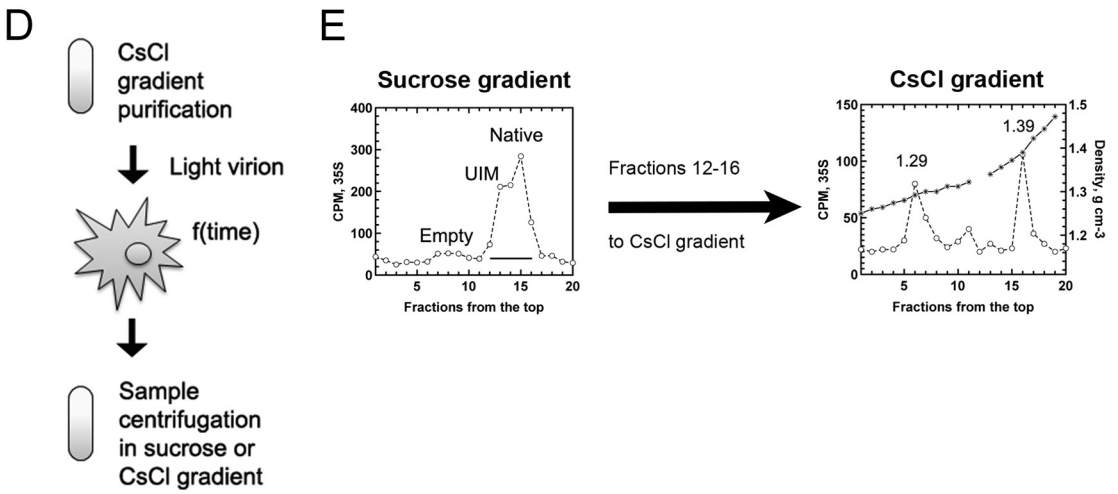

FIG 2 Dense-particle formation in cells during infection. (A) Gradient profiles of the *in vivo* conversion of native E1 (light particle, 1.28 to 1.29 g cm^{-3}) into dense particles (1.38 to 1.39 g cm^{-3}) in CsCl after 0, 30, 120, or 180 min postinfection. (B) Distribution of empty, light, and dense particles in CsCl gradients after incubation of light E1 on cells for 2 h or the addition of light E1 straight into the gradient. The results are averages from four replicates (± standard errors of the means). (C) Gradient profiles of the *in vivo* conversion of native E1 into uncoating intermediate particles (UIM) in a 5 to 20% sucrose gradient after 0, 30, 120, or 180 min postinfection. (D) Schematic image of the *in vivo* experiment in which the light fraction of CsCl-purified [^{35}S]methionine-cysteine-labeled E1 was collected and incubated on cells for the indicated amounts of time. Next, the collected cell homogenate was centrifuged in either a sucrose or a CsCl gradient. (E) After incubation on cells for 120 min, the cell homogenate was collected and centrifuged in a 5 to 20% sucrose gradient. Fractions 12 to 16 (indicated by a line) were collected from the sucrose gradient and subjected to a CsCl gradient.

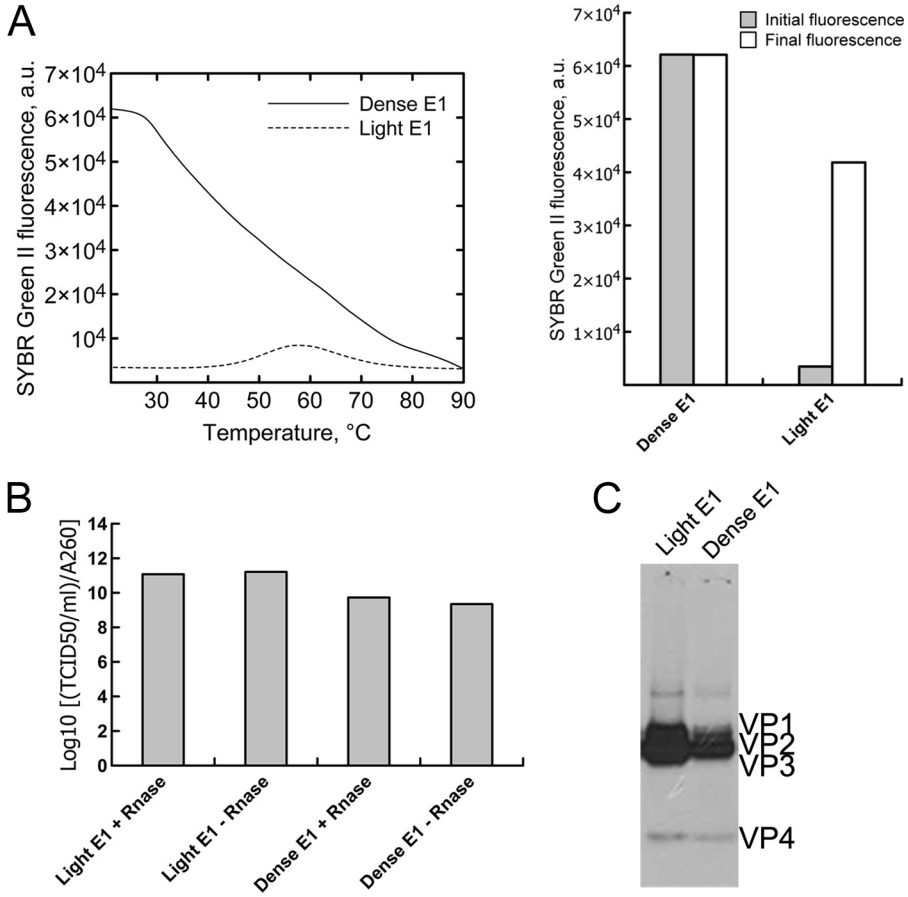

FIG 3 Capsid permeabilization and protein contents of light and dense E1 particles. (A) Thermal stability assay of dense E1 and light E1. The bar chart represents the initial and final absolute fluorescence values from thermal assay measurements. The final fluorescence value was measured after recooling of the sample back to 20°C. (B) Infectivity of light and dense E1 particles with or without RNase A treatment was determined with an endpoint dilution assay. The results are based on data from eight replicates for each sample. (C) ^{35}S-tagged dense and light E1 particles isolated from a CsCl gradient, separated via SDS-PAGE, and detected via autoradiography.

while the dense-particle band at 1.38 to 1.41 g cm^{-3} did not show any apparent increase in signal, indicating that heat conversion did not convert the native virions to the dense E1 particle. Additionally, a small band appeared at 1.22 g cm^{-3}, probably representing the empty virus particles. The absence of the main virion band signal can be explained by the repeated observation of a transparent "smudge" on the tube walls after the gradients had been fractioned, probably representing broken and aggregated virus particles (data not shown). Transmission electron microscopy (TEM) imaging showed that the native virion and the dense particles that naturally occur during E1 infection (Fig. 4B) share the morphology of an intact enterovirus. However, the heat-converted virions often showed an additional protrusion in the vicinity of the capsid (Fig. 4B), unlike the native and the dense E1 particles, further indicating structural differences between the heat-converted and dense E1 particles. It seems probable that the protrusion-showing particles were more open and more easily attracted to aggregations in the subsequent CsCl gradient. The quantification of the presence of protrusions in the heated particles showed that ~50% of the calculated 104 virus particles showed protrusions. Together, these results suggest that the naturally occurring dense particle cannot be formed by heating the virus to superphysiological temperatures, which also indicates that this type of heat treatment cannot be used to reliably monitor the uncoating of E1.

The dense particle is still highly infectious. The infectivity of the poliovirus 135S particle, as well as the altered particle of CVB3, was reported to be greatly reduced in cell cultures compared to the native virion (11, 37). Here, we investigated the dense particle in terms of its capacity to infect GMK cells within (i) a short time scale (Fig. 5A), (ii) an intermediate time scale (Fig. 5B), and (iii) a long time scale (Fig. 5C). All of the infectivity measurements were correlated by using comparable amounts of protein. In Fig. 5A, an antibody-based measurement of E1 infectivity (see Materials and Methods) was used to calculate the number of virus proteins produced in cells at 6 h postinfection. The titration of both the light and dense E1 particles showed a clear response to the decrease in the virus load used, indicating good sensitivity for this method. To evaluate infectivity over a long period of time (3 to 4 days), we determined the $TCID_{50}$ per milliliter for both light and dense E1 particles. Similarly to the antibody method, both light and dense E1 particles were capable of producing comparable levels of infection. Finally, we used a crystal violet-based method (see Materials and Methods) to determine infectivity at 24 h postinfection. We observed that all of the acquired data show high infection rates for

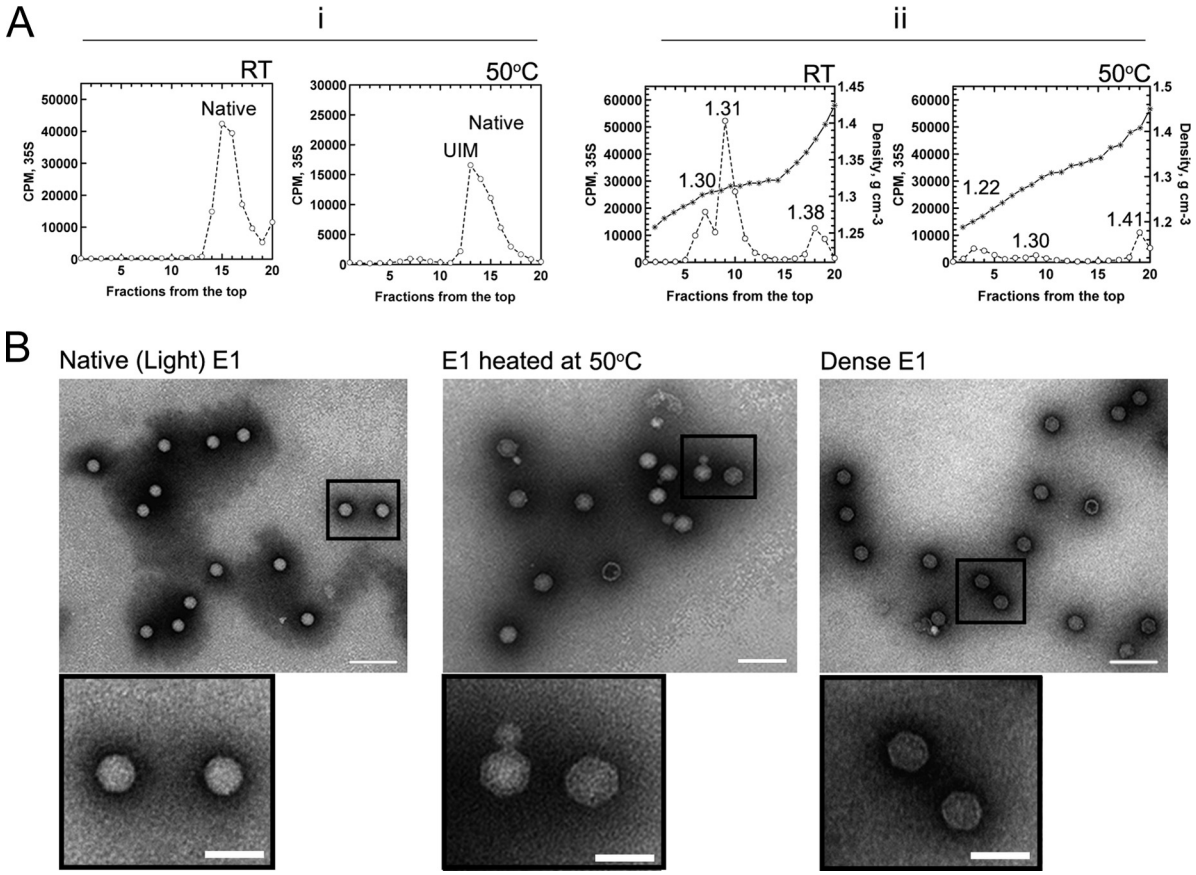

FIG 4 Heat conversion of [^{35}S]methionine-cysteine-labeled E1. (A) The virus was incubated at RT or 50°C for 5 min before loading either onto 5 to 20% sucrose (i) or into a CsCl gradient (ii). (B) Morphological evaluation of virus particles via transmission electron microscopy. The native virion (light), the E1 virion heated at 50°C, and dense E1 were negatively stained with 1% phosphotungstic acid before imaging. Bars, 100 nm and 25 nm for large images and blowups, respectively.

the dense E1 particle, although they were always slightly lower than those of the native virion.

The dense E1 particle is able to bind its receptor. The cell-induced conversion from the native to the altered 135S picornavirus particle is generally triggered by receptor-virion interactions. This type of particle conversion has been shown for at least poliovirus and rhinovirus (5), with both enteroviruses being considered model viruses in uncoating studies. Previous competition studies utilizing the E1 binding domain for its receptor $\alpha_2\beta_1$ integrin, the I-domain, showed that the I-domain is able to prevent the receptor-mediated cell attachment of E1 and that the I-domain alone is not able to initiate the uncoating process of E1 (32, 38). Here, we observed that the I-domain can push native E1 to higher melting temperatures in the presence of low I-domain-to-virion ratios (Fig. 6A), suggesting that the I-domain indeed can stabilize the E1 virion. The observed apparent T_m for E1 was ~53°C in the absence of any I-domain (Fig. 6A), whereas in the presence of the I-domain, the T_m increased by 3°C. We titrated the I-domain against 1 μg of E1 (Fig. 6A), starting from the first observable effective concentration, which corresponded to an I-domain-to-virion ratio of 10 (mole per mole), i.e., 100 ng of the I-domain. In our hands, the saturation point (maximum thermal stability induction by the I-domain) occurred at an I-domain-to-virion ratio of ~60 (mole/mole), that is, 500 ng of the I-domain. Previous studies using a similar I-domain–GST fusion protein suggested that up to five I-domain copies can occupy a single pentamer without any steric hindrance, resulting in a maximum of 60 I-domain copies per virion (32). Similarly to the previous report, the I-domain was able to block E1 infectivity (32). Here, we first incubated E1 with an I-domain–GST fusion protein for 1 h at 37°C prior to the addition of the virus to the cells. The infectivity of the light E1 particle was substantially blocked at an I-domain-to-virion ratio of ~50 (mole/mole) (Fig. 6B). This result was also reproducible with the dense E1 particle, although the I-domain seemed to be a more potent inhibitor at a lower I-domain concentration (Fig. 6B). Interestingly, previous studies on receptor-virion interactions using poliovirus and CVB3 indicated that the altered particle is likely to detach from its receptor (39, 40). By using TEM imaging, we studied whether the I-domain was able to bind both light and dense E1 fractions. After 1 h of incubation with the I-domain at 37°C, both the light and dense virions were clearly bound by several I-domain molecules, qualitatively supporting the observation that the dense E1 particle can bind to its receptor (Fig. 6C). This result also verified that the observed infection-blocking effect of the I-domain was due to capsid binding and not to virion disruption (Fig. 6C).

DISCUSSION

One of the hallmarks of the enterovirus genome delivery process is the generation of metastable uncoating intermediates. Upon ap-

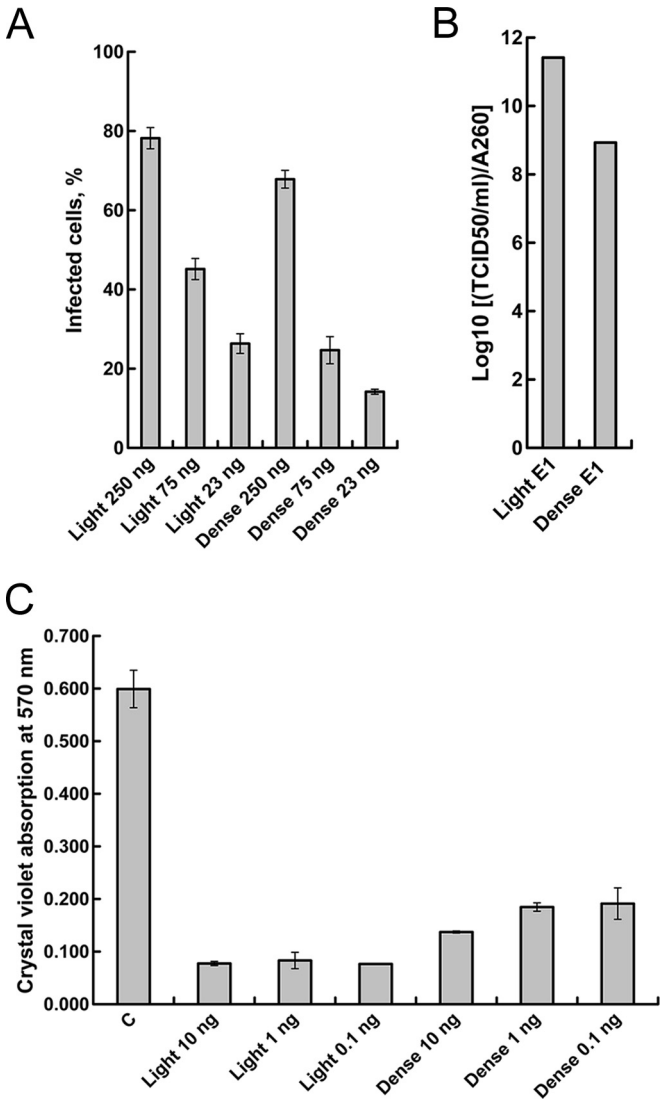

FIG 5 Infectivity of light and dense E1 particles. (A) The number of infected cells after 6 h postinfection was determined by immunolabeling the virus capsid and quantifying the number of infected cells based on confocal imaging. (B) The infectivity of E1 was determined with an endpoint titration assay, in which a dilution series of light or dense E1 with eight parallel dilutions was created. Infection was monitored for 3 days, after which infected cells were washed, and noninfected cells were stained to obtain the $TCID_{50}$ per milliliter (for more details, see Materials and Methods). (C) A CPE assay was used to determine infectivity at 24 h p.i. Three virus loads were used to infect cells: 10, 1, and 0.1 ng. After 24 h of infection, infected cells were washed, and noninfected cells were stained with crystal violet. The absorbance of crystal violet was measured with a microplate reader to evaluate the number of live cells. The results are averages of data from four replicates for each sample (± standard errors of the means).

propriate cues, the native virion is suggested to undergo a series of structural modifications, resulting in the loss of VP4, the externalization of the N-terminal sequence of VP1, and higher porosity, leading to the formation of an uncoating intermediate particle (6, 7). Depending on the enterovirus species, the native-to-altered-particle transition may be powered by a low pH (41) or receptor-virion interactions (42). In some cases, the receptor can serve as a capsid-stabilizing factor utilized only for cell surface attachment, as has been suggested by us and others previously regarding E1 and CVA9 (15, 23, 32, 43).

Here, we demonstrate the characteristics of another infectious, more open form of E1, which we identify as a possible uncoating intermediate particle of E1. This particle is found in cells during early infection and can be isolated by using CsCl gradient separation. In an effort to produce highly purified virus stocks, we found this dense particle when we ran the concentrated virus from a sucrose gradient in a CsCl gradient to further separate any possible impurities. The CsCl gradient separated two particle populations having markedly different buoyant densities (a light component, ~1.29 g cm^{-3}, and a dense component, ~1.37 g cm^{-3}). The commonly reported buoyant densities of the dense picornavirus preparations in CsCl were somewhat heavier, being around 1.44 g cm^{-3} for poliovirus and 1.44 to 1.47 g cm^{-3} for CVB5 and swine enterovirus (18–20). Similar to our findings for E1, the relative proportions of the dense and lighter intact populations for CVB5, poliovirus, or bovine enterovirus were not produced by the CsCl gradient itself, suggesting that the distributions of the two populations were faithful representations of their presence in virus preparations (18). In addition, we were able to show quantitatively that outside the cells, the native E1 virion is rather stable, whereas inside the cells, the dense particle is produced in large amounts after uptake.

Previous studies did not directly correlate the dense-particle populations in the CsCl gradient with the uncoating intermediate particles found after receptor-virion interactions. Here, in our study, we showed that the change in sucrose gradient sedimentation of the virus was correlated with the appearance of the dense-particle population in a CsCl gradient. The change was not evident on the cell surface but occurred after internalization at around 30 min p.i., which is in agreement with the uncoating time frame for poliovirus and for E1 (31, 44), suggesting that the observed dense E1 particle might be an uncoating intermediate. Additionally, when the broadened peak was collected from the sucrose gradient and subjected to CsCl gradient separation, both native particles and dense particles were observed. The minor change in the sucrose gradient was also explained via SDS-PAGE results, which showed that the VP4 protein was still mostly present in the dense particles. In our previous studies, we named the shoulder peak the 135S virion, as it was a dogma in the field that the 135S form is the intermediate form between the intact and empty forms (23, 45). However, in the light of the present data, it appears likely that the uncoating intermediate of E1 differs from those of some other enteroviruses and cannot be termed a true 135S particle, which has been shown to lack the VP4 protein (5). Therefore, we decided not to use this term but to use "uncoating intermediate particle" instead. Interestingly, previous studies on the dense poliovirus isolated from HeLa cells during infection showed the presence of VP4 using radioactive labeling, while silver staining could not detect VP4 for CVB5 or swine enterovirus (19, 20). This may reflect real differences in the presence of VP4 in the dense particle or differences in the sensitivities of the detection methods used (19, 20).

The large difference in the buoyant densities between the top and bottom components has been explained by a more open capsid structure that permits interactions between RNA and cesium. Data from our thermal assay experiments also suggest that the increased density is due to the capsid porosity in the case of the dense E1 particle. Previous reports using thermal assays with pi-

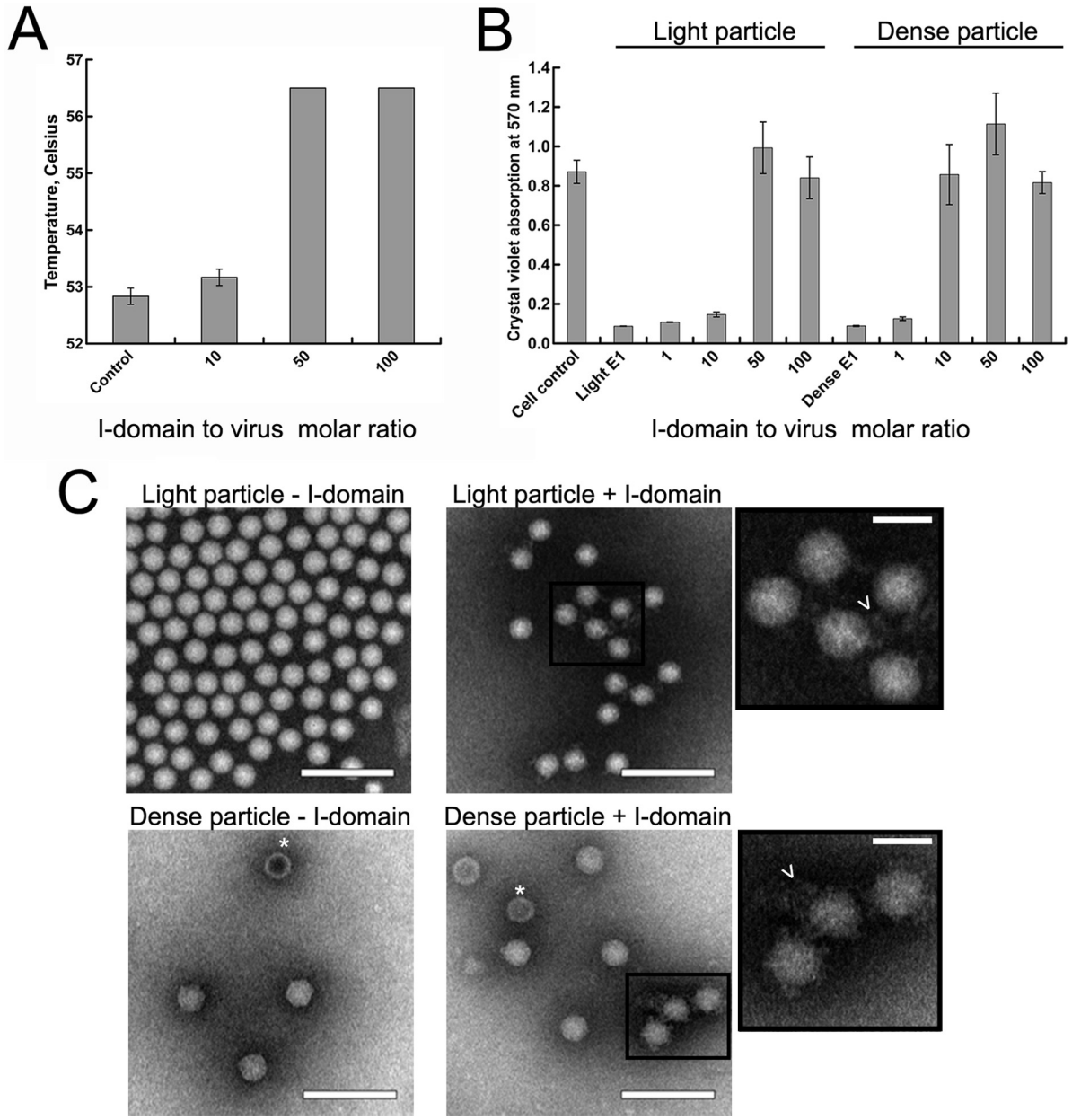

FIG 6 Receptor binding of light and dense E1 particles. (A) The melting temperature of E1 only (control) or with the I-domain was determined with a thermal assay in which SYBR green II was used as a reporter. (B) A competition assay was carried out to evaluate whether dense E1 could bind to the I-domain. Light or dense E1 was first incubated with four amounts of the I-domain for 1 h at 37°C, after which the virus was bound on cells for 1 h on ice. After washing the unbound virus, infection was allowed to proceed for 24 h at 37°C, after which infected cells were washed and noninfected cells were stained with crystal violet. The absorbance of crystal violet was measured with a microplate reader to evaluate the number of live cells. The results are averages of data from four replicates for each sample (± standard errors of the means). (C) The binding of the I-domain to E1 was also visualized via transmission electron microscopy. Light or dense E1 was incubated with or without the I-domain for 1 h at 37°C before addition to the grid and negative staining using phosphotungstic acid. The I-domain can be seen as hairy structures around the particles (arrowheads), and empty particles were also detected (asterisks). Bars, 100 nm and 25 nm for large images and blowups, respectively.

cornaviruses and SYBR green as a reporter molecule further showed that the 135S particles are permeable to small dye molecules (13). Additionally, it has been shown that native rhinovirus particles can permit dye access when incubated at 37°C, indicating that at a physiological temperature, the virus capsid may transition into a more dynamic state (46, 47). Here, we observed that the native E1 virion does not permit SYBR green II to penetrate the capsid structure at RT or 37°C, suggesting a tighter capsid structure than that of rhinovirus.

Heating of the native particles to superphysiological temperatures has been suggested to accurately mimic uncoating (37). However, the resulting profiles of such heat-converted enteroviruses in sucrose gradients have been shown to differ from one another, suggesting differences in their responses to heating and

difficulties in fully controlling the uncoating process by heating (48). Structural studies of A-particles have been performed mainly by heating native particles (12, 13, 16, 49) or by inducing particle alteration with a soluble receptor (11). In contrast to results for other enteroviruses, the heat conversion of native E1 virions differed from that of the E1 virions found in cells during infection. This was demonstrated by the fact that heating produced morphologically distinct particles with aberrant breakages, leading to a more extensive disruption in the subsequent CsCl gradients. The protrusions attached to the heated particles certainly suggest that the instability of the heated particles is linked to a different opening strategy than that of the particles derived from infected cells.

Previous reports suggest that upon conversion from the native virion to the altered 135S particles, there is a major loss in infectivity when the altered particles are used to infect cells *de novo* (37). This is not surprising given the fact that VP4 has been consistently shown to play a crucial role in the final genome delivery step, at least for poliovirus (8, 50). However, here, we demonstrate that dense E1 is not devoid of VP4, as was confirmed by radioactive detection. In addition, the slight shift in the virion peak in the sucrose gradient also suggests that only small changes in the virion structure occur during uncoating. Furthermore, we showed that dense E1 did not lose its ability to infect susceptible cells; rather, based on three well-established approaches to evaluate the infectivity of the particles, we confirmed the high infectivity of the dense particle.

In the cases of poliovirus and CVB3, receptor-induced 160S-to-135S conversion has been accompanied by the detachment of the virion-receptor complex (39, 40). Here, our biochemical and morphological experiments with the binding domain of the $\alpha_2\beta_1$ integrin receptor, the I-domain, did not apparently show lower levels of binding to the dense particle. The interaction between the receptor and dense E1 was also supported by infection experiments, where infection was determined after the dense virus was bound on ice and unbound virus was washed away. However, since the dense particle was shown to be a more open structure and slightly less infectious than the native virion, currently, it is possible that the change in the capsid structure might also have a small effect on receptor binding. Our previous studies on E1 suggested that the binding of the virus to its receptor $\alpha_2\beta_1$ integrin does not lead to extensive structural alterations in the E1 capsid, which is very similar to what was suggested previously for its close relative CVA9 (15, 32). Rather, these viruses are first transported to the endosomes, where, after some lag time, uncoating commences, leading to successful infection (27, 31). Importantly, we were able to confirm the previous assumption and directly show, using thermal assays, that receptor binding indeed stabilizes the native virus particle.

Conclusion. In conclusion, we have demonstrated that in addition to the native virus, another infectious E1 particle is found during infection. This particle has a more open structure and, hence, a higher buoyant density in CsCl gradients than the native virus. The dense particle still contains VP4 and is capable of binding to its receptor, and this binding leads to the stabilization of the virus particle and, later, to successful infection. Additionally, we show that this dense particle is distinct from the more fragile particle produced upon heat conversion.

ACKNOWLEDGMENTS

We thank Visa Ruokolainen for participating in the control experiments. We also thank Jyrki Heino for the GST–I-domain fusion and James Hogle for engaging in important discussions during this project.

FUNDING INFORMATION

This work, including the efforts of Mira Myllynen, Artur Kazmertsuk, and Varpu Marjomäki, was funded by Suomen Akatemia (Academy of Finland) (257125).

REFERENCES

1. **Monto AS.** 2002. Epidemiology of viral respiratory infections. Am J Med **112**(Suppl 6A):4S–12S.
2. **Hober D, Sauter P.** 2010. Pathogenesis of type 1 diabetes mellitus: interplay between enterovirus and host. Nat Rev Endocrinol **6:**279–289. http://dx.doi.org/10.1038/nrendo.2010.27.
3. **Roivainen M, Alfthan G, Jousilahti P, Kimpimäki M, Hovi T, Tuomilehto J.** 1998. Enterovirus infections as a possible risk factor for myocardial infarction. Circulation **98:**2534–2537. http://dx.doi.org/10.1161/01.CIR.98.23.2534.
4. **Laitinen OH, Honkanen H, Pakkanen O, Oikarinen S, Hankaniemi MM, Huhtala H, Ruokoranta T, Lecouturier V, Andre P, Harju R, Virtanen SM, Lehtonen J, Almond JW, Simell T, Simell O, Ilonen J, Veijola R, Knip M, Hyöty H.** 2014. Coxsackievirus B1 is associated with induction of beta-cell autoimmunity that portends type 1 diabetes. Diabetes **63:**446–455. http://dx.doi.org/10.2337/db13-0619.
5. **Tuthill TJ, Groppelli E, Hogle JM, Rowlands DJ.** 2010. Picornaviruses. Curr Top Microbiol Immunol **343:**43–89. http://dx.doi.org/10.1007/82_2010_37.
6. **Bergelson JM, Coyne CB.** 2013. Picornavirus entry. Adv Exp Med Biol **790:**24–41. http://dx.doi.org/10.1007/978-1-4614-7651-1_2.
7. **Paul AV, Schultz A, Pincus SE, Oroszlan S, Wimmer E.** 1987. Capsid protein VP4 of poliovirus is N-myristoylated. Proc Natl Acad Sci U S A **84:**7827–7831. http://dx.doi.org/10.1073/pnas.84.22.7827.
8. **Danthi P, Tosteson M, Li QH, Chow M.** 2003. Genome delivery and ion channel properties are altered in VP4 mutants of poliovirus. J Virol **77:**5266–5274. http://dx.doi.org/10.1128/JVI.77.9.5266-5274.2003.
9. **Brabec M, Schober D, Wagner E, Bayer N, Murphy RF, Blaas D, Fuchs R.** 2005. Opening of size-selective pores in endosomes during human rhinovirus serotype 2 in vivo uncoating monitored by single-organelle flow analysis. J Virol **79:**1008–1016. http://dx.doi.org/10.1128/JVI.79.2.1008-1016.2005.
10. **Pickl-Herk A, Luque D, Vives-Adrian L, Querol-Audi J, Garriga D, Trus BL, Verdaguer N, Blaas D, Caston JR.** 2013. Uncoating of common cold virus is preceded by RNA switching as determined by X-ray and cryo-EM analyses of the subviral A-particle. Proc Natl Acad Sci U S A **110:**20063–20068. http://dx.doi.org/10.1073/pnas.1312128110.
11. **Organtini LJ, Makhov AM, Conway JF, Hafenstein S, Carson SD.** 2014. Kinetic and structural analysis of coxsackievirus B3 receptor interactions and formation of the A-particle. J Virol **88:**5755–5765. http://dx.doi.org/10.1128/JVI.00299-14.
12. **Butan C, Filman DJ, Hogle JM.** 2014. Cryo-electron microscopy reconstruction shows poliovirus 135S particles poised for membrane interaction and RNA release. J Virol **88:**1758–1770. http://dx.doi.org/10.1128/JVI.01949-13.
13. **Ren J, Wang X, Hu Z, Gao Q, Sun Y, Li X, Porta C, Walter TS, Gilbert RS, Zhao Y, Axford D, Williams M, McAuley K, Rowlands DJ, Yin W, Wang J, Stuart DI, Rao Z, Fry EE.** 2013. Picornavirus uncoating intermediate captured in atomic detail. Nat Commun **4:**1929. http://dx.doi.org/10.1038/ncomms2889.
14. **Seitsonen JJ, Shakeel S, Susi P, Pandurangan AP, Sinkovits RS, Hyvönen H, Laurinmäki P, Yla-Pelto J, Topf M, Hyypiä T, Butcher SJ.** 2012. Structural analysis of coxsackievirus A7 reveals conformational changes associated with uncoating. J Virol **86:**7207–7215. http://dx.doi.org/10.1128/JVI.06425-11.
15. **Shakeel S, Seitsonen JJ, Kajander T, Laurinmäki P, Hyypiä T, Susi P, Butcher SJ.** 2013. Structural and functional analysis of coxsackievirus A9 integrin alphavbeta6 binding and uncoating. J Virol **87:**3943–3951. http://dx.doi.org/10.1128/JVI.02989-12.
16. **Shingler KL, Yoder JL, Carnegie MS, Ashley RE, Makhov AM, Conway JF, Hafenstein S.** 2013. The enterovirus 71 A-particle forms a gateway to

allow genome release: a cryoEM study of picornavirus uncoating. PLoS Pathog **9:**e1003240. http://dx.doi.org/10.1371/journal.ppat.1003240.
17. **Levy HC, Bostina M, Filman DJ, Hogle JM.** 2010. Catching a virus in the act of RNA release: a novel poliovirus uncoating intermediate characterized by cryo-electron microscopy. J Virol **84:**4426–4441. http://dx.doi.org/10.1128/JVI.02393-09.
18. **Rowlands DJ, Shirley MW, Sangar DV, Brown F.** 1975. A high density component in several vertebrate enteroviruses. J Gen Virol **29:**223–234. http://dx.doi.org/10.1099/0022-1317-29-2-223.
19. **Yamaguchi-Koll U, Wiegers KJ, Drzeniek R.** 1975. Isolation and characterization of 'dense particles' from poliovirus-infected HeLa cells. J Gen Virol **26:**307–319. http://dx.doi.org/10.1099/0022-1317-26-3-307.
20. **Urakawa T, Hamada N, Shingu M.** 1987. Isolation and antigenic characterization of dense particles of swine enteroviruses. Kurume Med J **34:**65–73. http://dx.doi.org/10.2739/kurumemedj.34.65.
21. **Cova-Baczko L, Aymard M.** 1982. Echovirus 11 dense particles: isolation and preliminary characterization. J Gen Virol **60:**159–163. http://dx.doi.org/10.1099/0022-1317-60-1-159.
22. **Wiegers KJ, Yamaguchi-Koll U, Drzeniek R.** 1977. Differences in the physical properties of dense and standard poliovirus particles. J Gen Virol **34:**465–473. http://dx.doi.org/10.1099/0022-1317-34-3-465.
23. **Marjomäki V, Pietiäinen V, Matilainen H, Upla P, Ivaska J, Nissinen L, Reunanen H, Huttunen P, Hyypiä T, Heino J.** 2002. Internalization of echovirus 1 in caveolae. J Virol **76:**1856–1865. http://dx.doi.org/10.1128/JVI.76.4.1856-1865.2002.
24. **Karjalainen M, Kakkonen E, Upla P, Paloranta H, Kankaanpää P, Liberali P, Renkema GH, Hyypiä T, Heino J, Marjomäki V.** 2008. A raft-derived, Pak1-regulated entry participates in alpha2beta1 integrin-dependent sorting to caveosomes. Mol Biol Cell **19:**2857–2869. http://dx.doi.org/10.1091/mbc.E07-10-1094.
25. **Karjalainen M, Rintanen N, Lehkonen M, Kallio K, Mäki A, Hellstrom K, Siljamäki V, Upla P, Marjomäki V.** 2011. Echovirus 1 infection depends on biogenesis of novel multivesicular bodies. Cell Microbiol **13:**1975–1995. http://dx.doi.org/10.1111/j.1462-5822.2011.01685.x.
26. **Liberali P, Kakkonen E, Turacchio G, Valente C, Spaar A, Perinetti G, Bockmann RA, Corda D, Colanzi A, Marjomäki V, Luini A.** 2008. The closure of Pak1-dependent macropinosomes requires the phosphorylation of CtBP1/BARS. EMBO J **27:**970–981. http://dx.doi.org/10.1038/emboj.2008.59.
27. **Soonsawad P, Paavolainen L, Upla P, Weerachatyanukul W, Rintanen N, Espinoza J, McNerney G, Marjomäki V, Cheng RH.** 2014. Permeability changes of integrin-containing multivesicular structures triggered by picornavirus entry. PLoS One **9:**e108948. http://dx.doi.org/10.1371/journal.pone.0108948.
28. **Huttunen M, Waris M, Kajander R, Hyypiä T, Marjomäki V.** 2014. Coxsackievirus A9 infects cells via nonacidic multivesicular bodies. J Virol **88:**5138–5151. http://dx.doi.org/10.1128/JVI.03275-13.
29. **Heikkilä O, Susi P, Tevaluoto T, Härmä H, Marjomäki V, Hyypiä T, Kiljunen S.** 2010. Internalization of coxsackievirus A9 is mediated by beta-2-microglobulin, dynamin, and Arf6 but not by caveolin-1 or clathrin. J Virol **84:**3666–3681. http://dx.doi.org/10.1128/JVI.01340-09.
30. **Marjomäki V, Turkki P, Huttunen M.** 2015. Infectious entry pathway of enterovirus B species. Viruses **7:**6387–6399. http://dx.doi.org/10.3390/v7122945.
31. **Siljamäki E, Rintanen N, Kirsi M, Upla P, Wang W, Karjalainen M, Ikonen E, Marjomäki V.** 2013. Cholesterol dependence of collagen and echovirus 1 trafficking along the novel alpha2beta1 integrin internalization pathway. PLoS One **8:**e55465. http://dx.doi.org/10.1371/journal.pone.0055465.
32. **Xing L, Huhtala M, Pietiäinen V, Käpylä J, Vuorinen K, Marjomäki V, Heino J, Johnson MS, Hyypiä T, Cheng RH.** 2004. Structural and functional analysis of integrin alpha2I domain interaction with echovirus 1. J Biol Chem **279:**11632–11638. http://dx.doi.org/10.1074/jbc.M312441200.
33. **Schmidtke M, Schnittler U, Jahn B, Dahse H, Stelzner A.** 2001. A rapid assay for evaluation of antiviral activity against coxsackie virus B3, influenza virus A, and herpes simplex virus type 1. J Virol Methods **95:**133–143. http://dx.doi.org/10.1016/S0166-0934(01)00305-6.
34. **Walter TS, Ren J, Tuthill TJ, Rowlands DJ, Stuart DI, Fry EE.** 2012. A plate-based high-throughput assay for virus stability and vaccine formulation. J Virol Methods **185:**166–170. http://dx.doi.org/10.1016/j.jviromet.2012.06.014.
35. **Garriga D, Pickl-Herk A, Luque D, Wruss J, Caston JR, Blaas D, Verdaguer N.** 2012. Insights into minor group rhinovirus uncoating: the X-ray structure of the HRV2 empty capsid. PLoS Pathog **8:**e1002473. http://dx.doi.org/10.1371/journal.ppat.1002473.
36. **Harutyunyan S, Kumar M, Sedivy A, Subirats X, Kowalski H, Kohler G, Blaas D.** 2013. Viral uncoating is directional: exit of the genomic RNA in a common cold virus starts with the poly-(A) tail at the 3′-end. PLoS Pathog **9:**e1003270. http://dx.doi.org/10.1371/journal.ppat.1003270.
37. **Curry S, Chow M, Hogle JM.** 1996. The poliovirus 135S particle is infectious. J Virol **70:**7125–7131.
38. **King SL, Cunningham JA, Finberg RW, Bergelson JM.** 1995. Echovirus 1 interaction with the isolated VLA-2 I domain. J Virol **69:**3237–3239.
39. **Lonberg-Holm K, Gosser LB, Kauer JC.** 1975. Early alteration of poliovirus in infected cells and its specific inhibition. J Gen Virol **27:**329–342. http://dx.doi.org/10.1099/0022-1317-27-3-329.
40. **Goodfellow IG, Evans DJ, Blom AM, Kerrigan D, Miners JS, Morgan BP, Spiller OB.** 2005. Inhibition of coxsackie B virus infection by soluble forms of its receptors: binding affinities, altered particle formation, and competition with cellular receptors. J Virol **79:**12016–12024. http://dx.doi.org/10.1128/JVI.79.18.12016-12024.2005.
41. **Prchla E, Kuechler E, Blaas D, Fuchs R.** 1994. Uncoating of human rhinovirus serotype 2 from late endosomes. J Virol **68:**3713–3723.
42. **Joklik WK, Darnell JE, Jr.** 1961. The adsorption and early fate of purified poliovirus in HeLa cells. Virology **13:**439–447. http://dx.doi.org/10.1016/0042-6822(61)90275-6.
43. **Rossmann MG, He Y, Kuhn RJ.** 2002. Picornavirus-receptor interactions. Trends Microbiol **10:**324–331. http://dx.doi.org/10.1016/S0966-842X(02)02383-1.
44. **Brandenburg B, Lee LY, Lakadamyali M, Rust MJ, Zhuang X, Hogle JM.** 2007. Imaging poliovirus entry in live cells. PLoS Biol **5:**e183. http://dx.doi.org/10.1371/journal.pbio.0050183.
45. **Pietiäinen V, Marjomäki V, Upla P, Pelkmans L, Helenius A, Hyypiä T.** 2004. Echovirus 1 endocytosis into caveosomes requires lipid rafts, dynamin II, and signaling events. Mol Biol Cell **15:**4911–4925. http://dx.doi.org/10.1091/mbc.E04-01-0070.
46. **Kremser L, Konecsni T, Blaas D, Kenndler E.** 2004. Fluorescence labeling of human rhinovirus capsid and analysis by capillary electrophoresis. Anal Chem **76:**4175–4181. http://dx.doi.org/10.1021/ac049842x.
47. **Kremser L, Petsch M, Blaas D, Kenndler E.** 2004. Labeling of capsid proteins and genomic RNA of human rhinovirus with two different fluorescent dyes for selective detection by capillary electrophoresis. Anal Chem **76:**7360–7365. http://dx.doi.org/10.1021/ac048999m.
48. **Airaksinen A, Somerharju P, Hovi T.** 2001. Variation in liposome binding among enteroviruses. Virology **279:**539–545. http://dx.doi.org/10.1006/viro.2000.0722.
49. **Bubeck D, Filman DJ, Cheng N, Steven AC, Hogle JM, Belnap DM.** 2005. The structure of the poliovirus 135S cell entry intermediate at 10-angstrom resolution reveals the location of an externalized polypeptide that binds to membranes. J Virol **79:**7745–7755. http://dx.doi.org/10.1128/JVI.79.12.7745-7755.2005.
50. **Panjwani A, Strauss M, Gold S, Wenham H, Jackson T, Chou JJ, Rowlands DJ, Stonehouse NJ, Hogle JM, Tuthill TJ.** 2014. Capsid protein VP4 of human rhinovirus induces membrane permeability by the formation of a size-selective multimeric pore. PLoS Pathog **10:**e1004294. http://dx.doi.org/10.1371/journal.ppat.1004294.